THE JOURNAL OF PHYSICAL CHEMISTRY Letters

pubs.acs.org/JPCL Letter

Local Carbon Concentration Determines the Graphene Edge Structure

Da Li, Yanchao Wang, Tian Cui,* Yanming Ma,* and Feng Ding*

Cite This: J. Phys. Chem. Lett. 2020, 11, 3451−3457 Read Online

ACCESS | Metrics & More | Article Recommendations | Supporting Information

ABSTRACT: Although the structures and properties of various graphene edges have attracted enormous attention, the underlying mechanism that determines the appearance of various edges is still unknown. Here, a global search of graphene edge structures is performed by using the particle swarm optimization algorithm. In addition to locating the most stable edges of graphene, two databases of graphene armchair and zigzag edge structures are built. Graphene edge self-passivation plays an important role in the stability of the edges of graphene, and self-passivated edge structures that contain both octagons and triangles are found for the first time. The obvious "apical dominance" feature of armchair edges is found. The appearance of the experimentally observed ac(56), ac(677), and Klein edges can be explained by the local carbon concentration. Additionally, the graphene edge database is also significant for the study of the open end of nanotubes or fullerenes.

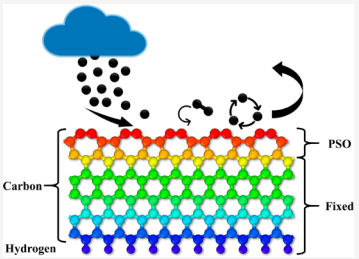

Similar to the surface of a 3D material, the edge geometry of a 2D material greatly affects the properties of the material and its applications.[1−4] The quasi-one-dimensional feature of the edge of a 2D material leads to unique physical properties and many potential applications in electronics and chemistry.[5] The structures and properties of the edges of graphene, the flagship 2D material, have attracted extensive attention.[6−17] The planar sp^2-hybridization of carbon atoms results in the highly stable ultraflat honeycomb lattice of graphene. Cutting the hexagonal lattice of graphene results in graphene nanoribbons or nanoflakes with either zigzag edges, armchair edges, or titled edges with both motifs (pristine edges).[18] In graphene, three sp^2-orbitals of a carbon atom form σ-bonds with three nearest-neighbor carbon atoms, while the remaining perpendicular p_z-orbital forms a delocalized π-bond with neighboring atoms. However, the cutting breaks σ-bonds and/or π-bonds at an edge of a graphene nanoribbon or nanoflake, and the carbon atoms at an edge have unsaturated or dangling bonds. The dangling bonds of carbon atoms at edges make the pristine edges of graphene highly unstable, with a formation energy of 2.0−3.0 eV per carbon atom.[19] In general, to stabilize the edge of graphene, the sp^2-orbital and π-orbital of a carbon atom at a graphene edge will be reorganized (self-passivated) or passivated by hydrogen atoms. Many studies have reported graphene edge reconstruction and passivation, and many edge structures have been proposed.[6,20−24] Instead of the pristine zigzag edge, the zz(57) edge, composed of a line of pentagon−heptagon pairs, was found to be the most stable zigzag-type edge, which was confirmed by experimental observations.[7,20,25] For the armchair edge, previous theoretical studies predicted that the experimentally observed ac(677) and ac(56) edges are metastable and that the ac(677) edge is just ∼0.1 eV/Å less stable than the pristine armchair edge, but the formation energy difference between the armchair edge and ac(56) edge is up to ∼0.5 eV/Å.[20] The edge formation energy difference between a pristine zigzag edge and the most stable zigzag edge, zz(57), is 0.35 eV/Å.[20] Girit et al. explored the stability and dynamics of the graphene edges of a hole.[7] Many different edges observed in this experiment were not considered in previous theoretical studies. To date, some fundamental properties, such as the magnetism of the zz(57) edge[26,27] and the migration and recombination of edge defects in zigzag nanoribbons, have been explored.[11,28,29] The reconstructed graphene edges, especially the Stone−Wales defects, have been fully investigated in theoretical and experimental studies.[11,22−24,28,30−36] The effect of a transition metal substrate on the stability of the graphene edge has been fully explored.[21,37−41]

However, to the best of our knowledge, a global search of the energy surface of the graphene edges is still missing, and therefore, many potential metastable structures have not been reported. Furthermore, some metastable edges, such as the ac(677) edge and the ac(56) edge, have been found in experiments. Therefore, these metastable edges are also experimentally interesting. The underlying mechanism that determines the appearance of a specific edge structure is still not clear. Molecular dynamics studies can reveal some edge structures but cannot be used to explore all possible edge

Received: February 17, 2020
Accepted: April 16, 2020
Published: April 16, 2020

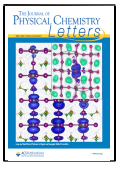

https://dx.doi.org/10.1021/acs.jpclett.0c00525
J. Phys. Chem. Lett. 2020, 11, 3451−3457

structures.[22,42,43] Considering the possible mass flow that appeared in previous experiments, such that carbon atoms could be knocked out by electron irradiation,[7,44−47] the local carbon concentration at an edge should be another important factor in addition to the thermodynamic stability that determines the appearance of the edge structure in real experiments.

In this Letter, we report a comprehensive theoretical study on the graphene edge structure using the particle swarm optimization (PSO) algorithm. The local carbon concentration at a graphene edge is considered a key factor in our global search. A database of graphene edges based on their minimal formation energies is constructed, and a diagram of the graphene edge formation energy versus local carbon concentration is obtained. Current results indicate that the appearance of the graphene edge is mainly determined by both the local carbon concentration and thermodynamic stability. The 16 most stable zigzag edges and thirty-six most stable armchair edges with various local carbon concentrations and their relative stabilities are predicted.

The calculations in this Letter are performed within the density functional theory (DFT) framework, carried out within the Vienna ab initio simulation package (VASP)[48,49] using the projector augmented wave method.[50] The C $2s^2 2p^2$ electrons and H $1s^1$ electrons are treated as valence electrons. For all calculations, the Perdew−Burke−Ernzerhof generalized gradient approximation (GGA) exchange and correlation functional is used.[51] Convergence tests give a kinetic energy cutoff of 400 eV, with a grid of spacing of $2\pi \times 0.03$ Å^{-1} for the electronic Brillouin zone (BZ) integration in all phases. The geometries are regarded as optimized when the remanent Hellmann−Feynman forces on the ions are less than 0.01 eV/Å. We choose the energies of graphene and H_2 as references.

To perform a global search of graphene edges, the PSO algorithm is employed to accelerate the exploration of the potential energy surface of graphene edges. The basic framework of edge structure prediction is based on the crystal structure analysis by particle swarm optimization (CALYPSO) method, which has been confirmed to be very efficient in the global structure prediction field.[52−54] To simplify the graphene edge prediction calculations, frozen nanoribbons with pristine zigzag (armchair) and hydrogen-terminated zigzag (armchair) edges are chosen as initial configurations in our calculations. The hydrogen atoms and the carbon atoms far from the exposed edge are fixed in the geometry optimization because the potential energy surface determined by this part remains constant; therefore, the expensive geometry optimization for this part is unnecessary. All the atoms near the edge are free to relax along all directions of the three-dimensional space. Additionally, periodic boundary conditions (PBCs) are used in the current study because PBCs can not only speed up calculations but also ensure good accuracy for the total energy calculations. The theoretically predicted periodic zz(57), ac(677), and ac(56) edges give a good description of the experimentally observed counterparts,[20,25] indicating that PBCs are very efficient. The graphene nanoribbon in our calculation is periodic in the y direction and separated by a vacuum region in the x and z directions, as shown in Figure 1a. The length of the vacuum region is greater than 15 Å to avoid the interaction between an edge and its periodic image. The possible size effect of graphene nanoribbons is omitted in the current study. The details of the edge structure prediction can be found in our previous study on the edge reconstruction of monolayer MoS_2. The stability of graphene edges is measured by the edge formation energy. In our nanoribbon models, a structure has two edges (reference edge and predicted edge). The reference edge is a hydrogen-terminated pristine zigzag or armchair edge (Figure 1b,c). The edge formation energy of the predicted edge can be calculated by the following formula:

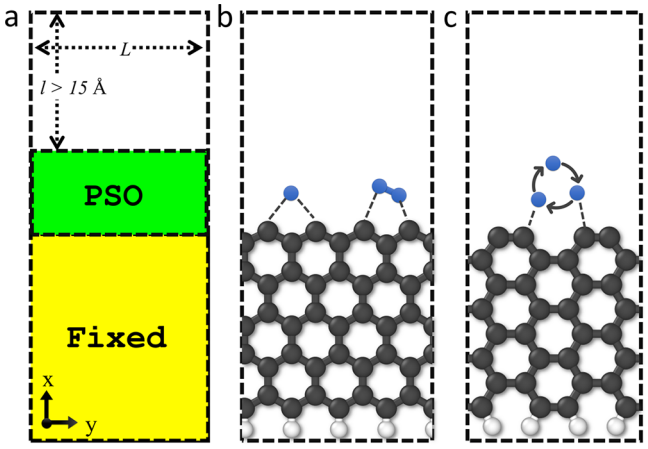

Figure 1. (a) Schematic of the theoretical model for graphene edge prediction and the frozen structural models of pristine hydrogen-terminated (b) zigzag and (c) armchair edges of graphene. The black and white spheres represent carbon and hydrogen atoms, respectively. The blue spheres represent the carbon atoms operated on by the PSO algorithm.

$$E_{edge} = \frac{1}{L}\left(E_t - N_c E_{Gr} - \frac{1}{2} N_h E_{H_2}\right) - E_{ref}$$

where E_t, E_{Gr}, and E_{H_2} are the total energies of the graphene nanoribbon, graphene, and H_2 molecules, respectively. N_c and N_h are the numbers of carbon and hydrogen atoms in the graphene nanoribbon, respectively. E_{ref} is the edge formation energy of the hydrogen-terminated zigzag edge or armchair edge. L is the length of the graphene nanoribbon in the y direction. E_{ref} is obtained from a symmetrized graphene nanoribbon that contains two hydrogen-terminated zigzag or armchair edges. E_{edge} and E_{ref} are in units of eV/Å. In the global search of graphene edge prediction, the local carbon concentration is considered a key factor. The local carbon concentration can be described as $C_l = (N_c - N_{pristine})/L$, where $N_c - N_{pristine}$ is the number of added carbon atoms in each calculation. Considering the interatomic distance (∼1.42 Å) and the sp^2-hybridization feature of graphene,[7] a carbon concentration in the range of 0−1.4 atoms/Å is chosen to fully explore the potential energy surface of the configuration space of the graphene edge. We use 1−4 unit cells to perform the edge structure prediction. For each carbon concentration, approximately 2000 candidate edge structures are calculated. The experimentally observed zz(57), ac(56), ac(677), and Klein edges[25] are predicted in our calculation, indicating the feasibility and accuracy of the current model and simulation parameters. The entire edge databases of graphene that contain 37 zigzag edges and 78 armchair edges are shown in Figures S1 and S2, and the edge formation energies are shown in Table S1. We should note that some carbon atoms of some optimized structures are out of the plane of the graphene bulk, such as the apex atoms in the zz28 and ac21 edges (Figure S3). Exploring structures with very large supercells is beyond the capacity of DFT study, but we anticipate that the

https://dx.doi.org/10.1021/acs.jpclett.0c00525
J. Phys. Chem. Lett. 2020, 11, 3451−3457

most stable ones can be regarded as a combination of different edges obtained in the current database.

Figure 2 presents the edge configurational energy spectra of the zigzag and armchair edges of graphene. The candidate edge

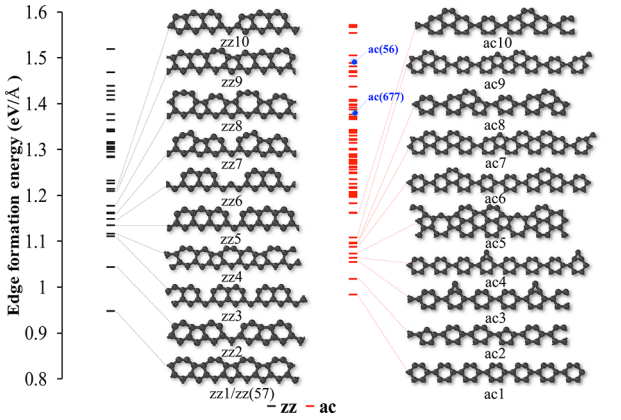

Figure 2. Configurational energy spectra of the zigzag and armchair edges of graphene. The inset in each column illustrates the 10 most stable zigzag or armchair edges. The edge formation energies of the experimentally observed ac(56) and ac(677) edges are highlighted by blue points.

structures with edge formation energies between 0.9 and 1.6 eV/Å are chosen to construct two databases of the zigzag and armchair edges of graphene. In addition to the pristine zigzag edge and armchair edge, 37 zigzag-type edges and 77 armchair-type edges are predicted in the current global search. The experimentally observed ac(677) and ac(56) edges are also confirmed in the current global search. To investigate the stability mechanism of graphene edges, the 10 most stable zigzag and armchair edges are selected, as shown in Figure 2. The most stable zigzag edge is still the zz(57) edge (zz1), which was reported in both theoretical and experimental studies.[20,25] The calculated difference in the edge formation energies between the zz(57) edge and pristine zigzag edges is 0.34 eV/Å, which is in very good agreement with the value (0.35 eV/Å) in a previous study,[20] indicating the efficiency of our edge formation energy calculations. In addition to the most stable zz(57) edge, the nine other edge structures are reported for the first time. The building blocks at zigzag terraces of zigzag-type edges are pentagons, hexagons, heptagons, and octagons. The zigzag terraces of some (zz2, zz3, zz5, zz6, zz7, and zz10) of the 10 most stable zigzag edges are not fully occupied by polygons. Some kink sites occur at the zigzag terraces that are composed of polygon alignments such as hexagon−pentagon−hexagon (6|5|6) alignments, hexagon−hexagon (6|6) pairs, hexagon−hexagon−hexagon (6|6|6) alignments, heptagon−pentagon−hexagon (7|5|6) alignments, and pentagon−hexagon−hexagon (5|6|6) alignments. In contrast, the zigzag terraces of the zz1, zz4, zz8, and zz9 edges are fully occupied by polygons. Interestingly, a common feature is found. The building blocks of these four edges are completely or partially pentagon−heptagon (5|7) pairs. The sequences of polygons at the zz1, zz4, zz8, and zz9 edges are 5|7, 5|7|6, 5|7|5|8, and 5|7|6|6, respectively. The zz8 edge can be regarded as a carbon-rich zz1 (zz(57)) edge and is composed of two pentagons, one heptagon, and one octagon. Notably, the zz7 and zz8 edges exhibit three carbon atom linear arrangements not reported in the literature. According to our database of zigzag edges, although the zz(57) edge is the most stable zigzag edge, the edges composed of isolated pentagon−heptagon pairs (zz18 and zz29) are not stable in energy. For armchair-type edges, the pristine armchair edge is still the most stable edge. The building blocks of the 10 most stable armchair edges are triangles, pentagons, hexagons, and heptagons. Unexpectedly, the triangle can stabilize the armchair edges (ac3 and ac4). According to our database of armchair edges, the armchair-type edges have an obvious "apical dominance" effect. The carbon atoms tend to stack up instead of being horizontally arranged (ac5−10). This result also confirms that the zigzag edge-extended graphene nanoribbons (zeeGNRs) have higher stability and are easily obtained.[12] Furthermore, the experimentally observed ac(56) and ac(677) edges do not have a good advantage in energy.

Edge self-passivation is a very important factor for the stability of graphene edges.[20] The electron localization function calculations indicate that the outermost carbon atoms for the most stable zz(57) and pristine armchair edges form perfectly self-passivated two-carbon-atom units (C_2 units) (Figure S4). The electrons in the C_2 units are greatly localized and form strong covalent bonds. The second stable zigzag edge zz2 (polygon arrangement: zz(0656)) can be regarded as reconstructed zz(0606). Two neighboring hexagons of zz(0606) become close and form a pentagon to balance the interaction of the dangling bonds of the hexagons. In the zz2 edge, self-passivated C_2 units appear at the shoulder of the 6|5|6 alignments. The electrons in the C_2 units form strong localized covalent bonds. In the zz3 edge, the electrons of C_2 units at the shoulder of the 6|6 pairs form strong localized covalent bonds. Strong Coulomb repulsion occurs between two neighboring 6|6 pairs. Two neighboring hexagons do not need to combine because the dangling bonds are already balanced. A similar self-passivation of C_2 units can also be observed for the zz5 and zz6 edges. The dangling bonds of the carbon atoms in the middle of the 6|6|6 alignment of zz5 form isolated electron pairs that are also protected by the self-passivated C_2 units of the 6|6|6 alignment. In the zz4 and zz9 edges, the isolated electron pairs are also isolated and protected by two neighboring self-passivated C_2 units of heptagons. In the zz7 and zz8 edges, the unbonded electrons of the middle atom in the linear three-atom units transform into two neighboring carbon atoms and balance the dangling bond of this atom. In the zz10 edge, the electrons of carbon atoms at the shoulder of the 5|6|6 alignments are strongly localized. Except for the strong covalent bonds of C_2 units, the electrons of dangling bonds of carbon atoms in the pentagon and neighboring hexagon form isolated electron pairs. For armchair edges, the presence of self-passivated C_2 units is also the most common feature of the most stable edges. The ac1 edge (pristine armchair edge) is the most stable edge because its structure has perfect self-passivation features. All the electrons in C_2 units are strongly localized. With the presence of "zigzag" atoms, the edge becomes unstable. In the ac2, ac7, ac8, and ac9 edges, some pentagons have dangling bonds that need to be balanced. The triangles of the ac3 and ac4 edges were not reported in previous studies. The carbon atom at the top of the triangle has dangling bonds, which make the structure unstable. The ac5 edge has inverse 5|7 pairs with dangling bonds. For the ac6, ac8, and ac10 edges, although the edge structures are covered by C_2 units, an obvious "apical dominance" effect is observed for these structures. "Zigzag"

https://dx.doi.org/10.1021/acs.jpclett.0c00525
J. Phys. Chem. Lett. 2020, 11, 3451−3457

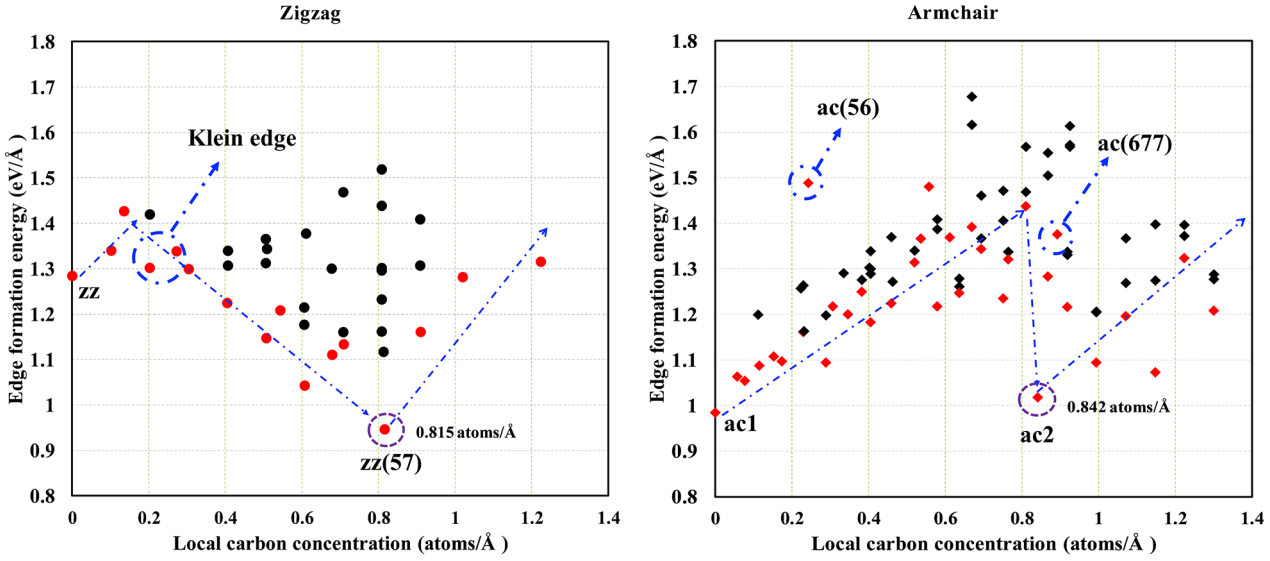

Figure 3. Edge formation energies of zigzag and armchair edges as a function of the local carbon concentration. The most stable edge at a specific local carbon concentration is highlighted in red. Solid circles and squares indicate the zigzag and armchair edges, respectively.

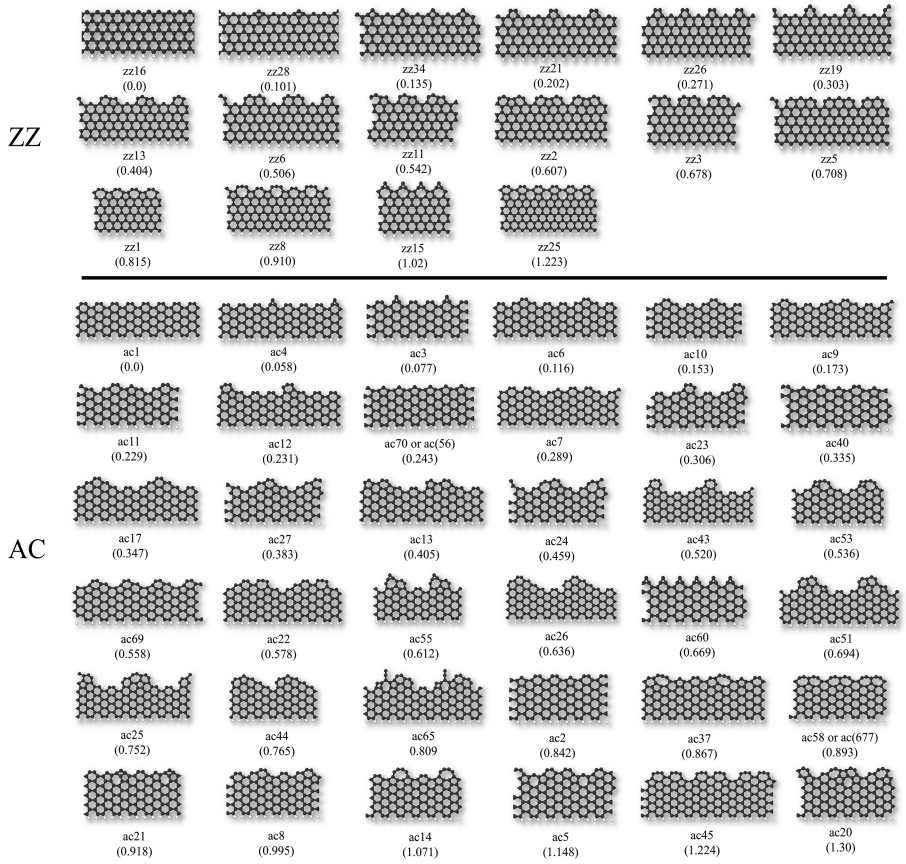

Figure 4. Most stable structures of the zigzag and armchair edges at various local carbon concentrations (in atoms/Å). The edges are organized in order of local carbon concentration. The value in the parentheses is the local carbon concentration of each edge.

atoms appear at the shoulder of the 6|6|6 alignments. These "zigzag" atoms have dangling bonds that need to be balanced.

The thermodynamic stability is very critical for the existence of a graphene edge. However, it is not the only factor that determines the appearance of an edge in experiments. The experimentally observed ac(677) and ac(56) edges also confirm this point because they are metastable in our database, as shown in Figure 2. Furthermore, the gap between the edge formation energies of the most stable pristine armchair edge and the experimentally observed ac(677) or ac(56) edge is larger than that of other edges, indicating that many candidate structures in our database could also appear in experiments. Although the hydrogen-terminated ac(677), ac(56), and zz(57) edges have been used to explain the changes in the

https://dx.doi.org/10.1021/acs.jpclett.0c00525
J. Phys. Chem. Lett. 2020, 11, 3451−3457

thermodynamic stabilities of the ac(677), ac(56), and zz(57) edges under hydrogenation,[20] the reason for observing the ac(677), ac(56), zz(57), and Klein edges at the same time in experiments cannot be fully understood. Considering the possible mass flow that appeared in previous experiments, such that carbon atoms could be knocked out by electron irradiation,[7,44−47] the local carbon concentration at an edge should be another important factor in addition to the thermodynamic stability that determines the appearance of an edge in experiments. The experimentally observed ac(677), ac(56), and zz(57) edges have different local carbon concentrations of 0.893, 0.243, and 0.815 atoms/Å, respectively. Therefore, we have reorganized our energy-based zigzag and armchair edge databases to best show the effect of the local carbon concentration on the appearance of an edge. The established edge formation energy versus local carbon concentration diagrams of the zigzag and armchair edges of graphene are shown in Figure 3. The most stable edges at various carbon concentrations are used to construct the local carbon concentration-based graphene edge databases, as shown in Figure 4. The edge formation energies versus local carbon concentration diagrams roughly have linear trends in some carbon concentration ranges without considering the energy undulation induced by the complex chemical interactions.

For zigzag-type edges, the edge formation energies also have some undulations with increasing local carbon concentration, as shown in Figure 3. The whole process can be divided into three stages. The edge formation energies of the most stable edges at various local concentrations first increase, then sharply decrease, and finally increase again. In the first stage, the local carbon concentration (zz28: 0.101 atoms/Å ∼ zz34: 0.135 atoms/Å) is very low, and the carbon atoms are located in the middle of two neighboring carbon atoms on zigzag terraces. As the local carbon concentration increases, the isolated carbon atoms on zigzag terraces undergo a transition of recombination with other carbon atoms to form a Klein edge (zz21: 0.202 atoms/Å ∼ zz26: 0.271 atoms/Å). At this stage, the edge formation energies of the most stable zigzag edges considerably decrease. The Klein edges further transform into edges composed of isolated hexagons (zz19: 0.303 atoms/Å). These hexagons have a Jahn−Teller distortion that balances the edge stress. Then, the distorted hexagons transform into the kink edge composed of hexagon−pentagon (6|5) pairs at a local carbon concentration of 0.404 atoms/Å. The 6|5 pairs further transform into 6|6 pairs at a local carbon concentration of 0.506 atoms/Å (zz6). Then, the kink edge with 6|5 pairs (zz11: 0.542 atoms/Å) appears. As the local carbon concentration increases, the 6|5 pairs on the zigzag terrace transform into hexagon−pentagon−hexagon (6|5|6) alignments (zz2: 0.607 atoms/Å), then into two 6|6 pairs (zz3: 0.678 atoms/Å), and further into 6|6|6 alignments (zz5: 0.708 atoms/Å). Interestingly, 0.815 atoms/Å (zz1: 0.815 atoms/Å) is found to be a critical value that corresponds to the most stable zigzag edge zz(57) (zz1). When the local carbon concentration is greater than this value, the transition enters the third stage. At this stage, the local carbon concentration is over-rich concerning the local carbon concentration of the most stable zz(57) edge. The 5|7 pairs transform into pentagon−heptagon−pentagon−octagon (5|7|5|8) alignments (zz8: 0.910 atoms/Å), then into the 5|7 pairs with a triangle at the top of the pentagon (zz15: 1.02 atoms/Å), and further into the 5|7 pairs with a hexagon at the top of the pentagon (zz25: 1.223 atoms/Å). The carbon-rich condition results in a spontaneous transition from zigzag-type edges to armchair-type edges.

For armchair-type edges, the edge formation energy versus local carbon concentration diagram also has obvious transitions with changing local carbon concentration. However, the variation trend is very different from that for zigzag-type edges. The pristine armchair edge has the lowest formation energy, induced by the perfect self-passivation of carbon atoms. With increasing carbon concentration, the added carbon atoms on the armchair terrace destroy the perfect self-passivation of the pristine armchair edge. The edge formation energy linearly increases with increasing local carbon concentration without considering the energy undulation induced by interatomic interactions. Then, a very sharp decrease appears at a local carbon concentration of 0.842 atoms/Å. Finally, the edge formation energy increases again. Different from zigzag-type edges, triangles appear at armchair-type edges at low local carbon concentrations (ac4: 0.058 atoms/Å; ac3: 0.077 atoms/Å). The experimentally observed ac(56) edge appears at a local carbon concentration of 0.243 atoms/Å. When the local carbon concentration is in the range of 0.335−0.842 atoms/Å, the obvious "apical dominance" effect can be observed in the armchair edge structures. The edges in this range tend to form isolated "peaks". The edge formation energy of the ac2 edge at a local carbon concentration of 0.842 atoms/Å is a local minimum. The energy difference between the ac2 edge and the pristine armchair edge (ac1) is only 0.03 eV/Å, indicating that the ac2 edge has a high chance to easily revert to the most stable pristine armchair edge. Furthermore, the local carbon concentration of 0.842 atoms/Å (ac2) is a critical value for the armchair-type edges. When the local carbon concentration is greater than this value, the "apical dominance" effect becomes less obvious. The experimentally observed ac(677) edge appears in this range.

Next, we study the electronic structures of the graphene nanoribbons composed of the local carbon concentration-determined zigzag and armchair edges (Figures S5−S58). The graphene nanoribbons composed of the 16 most stable local carbon concentration-determined zigzag edges are metallic. Only the graphene nanoribbon composed of the carbon-rich zz25 edge is a narrow bandgap semiconductor. The armchair nanoribbons composed of 17 armchair edges (ac1, ac4, ac3, ac70, ac40, ac43, ac55, ac26, ac60, ac25, ac44, ac65, ac2, ac58, ac21, ac14, and ac5) in our database are semiconductors. The other 19 edges are metallic.

In summary, we extensively explored the potential energy surfaces of graphene edges by using the PSO algorithm. The highly stable edge structures of graphene with various local carbon concentrations are predicted. Our global search enables the construction of two databases of the graphene edge for the first time, which include 37 zigzag edges and 78 armchair edges. The structural evolution of graphene edges under various local carbon concentrations is explored. Some unique self-passivated edges that contain octagons or triangles are uncovered for the first time. An obvious "apical dominance" feature of armchair edges is found. The "zigzag" atoms appearing at the shoulder of the peaks of armchair edges destroy the stability of pristine armchair edges because of the presence of unpassivated dangling bonds. On the basis of our databases, the local carbon concentration is confirmed to be another important factor in the appearance of graphene edges in addition to the thermodynamic stability. The two

https://dx.doi.org/10.1021/acs.jpclett.0c00525
J. Phys. Chem. Lett. 2020, 11, 3451−3457

reorganized local carbon concentration-based databases of graphene edges contain the 16 most likely zigzag edges and 36 most likely armchair edges, which can be found in experiments. These two local carbon concentration-determined databases can explain the appearance of the experimentally observed ac(56), ac(677), zz(57), and Klein edges very well. The graphene edge databases are significant for the study of the open end of nanotubes or fullerenes and are a good reference for future experiments.

■ ASSOCIATED CONTENT

Supporting Information

The Supporting Information is available free of charge at https://pubs.acs.org/doi/10.1021/acs.jpclett.0c00525.

Whole edge database of graphene, details of edges zz28 and ac21, electronic localization function, and electronic band structures (PDF)

■ AUTHOR INFORMATION

Corresponding Authors

Tian Cui − *State Key Lab of Superhard Materials, College of Physics, Jilin University, Changchun 130012, P.R. China; School of Physical Science and Technology, Ningbo University, Ningbo 315211, P.R. China;* orcid.org/0000-0002-9664-848X; Email: cuitian@jlu.edu.cn

Yanming Ma − *State Key Lab of Superhard Materials, College of Physics, Jilin University, Changchun 130012, P.R. China;* Email: mym@jlu.edu.cn

Feng Ding − *Center for Multidimensional Carbon Materials, Institute for Basic Science (IBS), Ulsan 44919, Republic of Korea; Department of Materials Science and Engineering, Ulsan National Institute of Science and Technology (UNIST), Ulsan 44919, Republic of Korea;* orcid.org/0000-0001-9153-9279; Email: f.ding@unist.ac.kr

Authors

Da Li − *State Key Lab of Superhard Materials, College of Physics, Jilin University, Changchun 130012, P.R. China; Center for Multidimensional Carbon Materials, Institute for Basic Science (IBS), Ulsan 44919, Republic of Korea;* orcid.org/0000-0002-0041-9181

Yanchao Wang − *State Key Lab of Superhard Materials, College of Physics, Jilin University, Changchun 130012, P.R. China;* orcid.org/0000-0003-4518-925X

Complete contact information is available at: https://pubs.acs.org/10.1021/acs.jpclett.0c00525

Notes

The authors declare no competing financial interest.

■ ACKNOWLEDGMENTS

D.L. acknowledges support from National Natural Science Foundation of China (91745203 and 11404134). F.D. acknowledges support from the Institute for Basic Science (IBS-R019-D1) of South Korea and the computational resources from CMCM, IBS.

■ REFERENCES

(1) Batzill, M. The Surface Science of Graphene: Metal Interfaces, Cvd Synthesis, Nanoribbons, Chemical Modifications, and Defects. *Surf. Sci. Rep.* **2012**, *67*, 83−115.

(2) Zhong, Y.; Zhen, Z.; Zhu, H. Graphene: Fundamental Research and Potential Applications. *FlatChem.* **2017**, *4*, 20−32.

(3) Rasool, H. I.; Ophus, C.; Zettl, A. Atomic Defects in Two Dimensional Materials. *Adv. Mater.* **2015**, *27*, 5771−5777.

(4) Acik, M.; Chabal, Y. J. Nature of Graphene Edges: A Review. *Jpn. J. Appl. Phys.* **2011**, *50*, 070101.

(5) Bellunato, A.; Arjmandi Tash, H.; Cesa, Y.; Schneider, G. F. Chemistry at the Edge of Graphene. *ChemPhysChem* **2016**, *17*, 785−801.

(6) Kim, K.; Coh, S.; Kisielowski, C.; Crommie, M. F.; Louie, S. G.; Cohen, M. L.; Zettl, A. Atomically Perfect Torn Graphene Edges and Their Reversible Reconstruction. *Nat. Commun.* **2013**, *4*, 2723.

(7) Girit, Ç. Ö.; Meyer, J. C.; Erni, R.; Rossell, M. D.; Kisielowski, C.; Yang, L.; Park, C.-H.; Crommie, M. F.; Cohen, M. L.; Louie, S. G.; et al. Graphene at the Edge: Stability and Dynamics. *Science* **2009**, *323*, 1705.

(8) Suenaga, K.; Koshino, M. Atom-by-Atom Spectroscopy at Graphene Edge. *Nature* **2010**, *468*, 1088−1090.

(9) He, K.; Lee, G.-D.; Robertson, A. W.; Yoon, E.; Warner, J. H. Hydrogen-Free Graphene Edges. *Nat. Commun.* **2014**, *5*, 3040.

(10) Liu, Z.; Lin, Y.-C.; Lu, C.-C.; Yeh, C.-H.; Chiu, P.-W.; Iijima, S.; Suenaga, K. In Situ Observation of Step-Edge in-Plane Growth of Graphene in a Stem. *Nat. Commun.* **2014**, *5*, 4055.

(11) He, K.; Robertson, A. W.; Fan, Y.; Allen, C. S.; Lin, Y.-C.; Suenaga, K.; Kirkland, A. I.; Warner, J. H. Temperature Dependence of the Reconstruction of Zigzag Edges in Graphene. *ACS Nano* **2015**, *9*, 4786−4795.

(12) Beyer, D.; Wang, S.; Pignedoli, C. A.; Melidonie, J.; Yuan, B.; Li, C.; Wilhelm, J.; Ruffieux, P.; Berger, R.; Müllen, K.; et al. Graphene Nanoribbons Derived from Zigzag Edge-Encased Poly(Para-2,9-Dibenzo[Bc/Kl]Coronenylene) Polymer Chains. *J. Am. Chem. Soc.* **2019**, *141*, 2843−2846.

(13) Yamada, Y.; Kawai, M.; Yorimitsu, H.; Otsuka, S.; Takanashi, M.; Sato, S. Carbon Materials with Zigzag and Armchair Edges. *ACS Appl. Mater. Interfaces* **2018**, *10*, 40710−40739.

(14) Zhang, X.; Xin, J.; Ding, F. The Edges of Graphene. *Nanoscale* **2013**, *5*, 2556−2569.

(15) Ma, T.; Ren, W. C.; Zhang, X. Y.; Liu, Z. B.; Gao, Y.; Yin, L. C.; Ma, X. L.; Ding, F.; Cheng, H. M. Edge-Controlled Growth and Kinetics of Single-Crystal Graphene Domains by Chemical Vapor Deposition. *Proc. Natl. Acad. Sci. U. S. A.* **2013**, *110*, 20386−20391.

(16) Tian, J.; Cao, H.; Wu, W.; Yu, Q.; Chen, Y. P. Direct Imaging of Graphene Edges: Atomic Structure and Electronic Scattering. *Nano Lett.* **2011**, *11*, 3663−3668.

(17) Singh, V.; Joung, D.; Zhai, L.; Das, S.; Khondaker, S. I.; Seal, S. Graphene Based Materials: Past, Present and Future. *Prog. Mater. Sci.* **2011**, *56*, 1178−1271.

(18) Liu, Y.; Dobrinsky, A.; Yakobson, B. I. Graphene Edge from Armchair to Zigzag: The Origins of Nanotube Chirality? *Phys. Rev. Lett.* **2010**, *105*, 235502.

(19) Hyun, C.; Yun, J.; Cho, W. J.; Myung, C. W.; Park, J.; Lee, G.; Lee, Z.; Kim, K.; Kim, K. S. Graphene Edges and Beyond: Temperature-Driven Structures and Electromagnetic Properties. *ACS Nano* **2015**, *9*, 4669−4674.

(20) Koskinen, P.; Malola, S.; Häkkinen, H. Self-Passivating Edge Reconstructions of Graphene. *Phys. Rev. Lett.* **2008**, *101*, 115502.

(21) Gao, J.; Zhao, J.; Ding, F. Transition Metal Surface Passivation Induced Graphene Edge Reconstruction. *J. Am. Chem. Soc.* **2012**, *134*, 6204−6209.

(22) Kroes, J. M. H.; Akhukov, M. A.; Los, J. H.; Pineau, N.; Fasolino, A. Mechanism and Free-Energy Barrier of the Type-57 Reconstruction of the Zigzag Edge of Graphene. *Phys. Rev. B: Condens. Matter Mater. Phys.* **2011**, *83*, 165411.

(23) Rodrigues, J. N. B.; Gonçalves, P. A. D.; Rodrigues, N. F. G.; Ribeiro, R. M.; Lopes dos Santos, J. M. B.; Peres, N. M. R. Zigzag Graphene Nanoribbon Edge Reconstruction with Stone-Wales Defects. *Phys. Rev. B: Condens. Matter Mater. Phys.* **2011**, *84*, 155435.

(24) Wagner, P.; Ivanovskaya, V. V.; Melle-Franco, M.; Humbert, B.; Adjizian, J.-J.; Briddon, P. R.; Ewels, C. P. Stable Hydrogenated

Graphene Edge Types: Normal and Reconstructed Klein Edges. *Phys. Rev. B: Condens. Matter Mater. Phys.* **2013**, *88*, 094106.
(25) Koskinen, P.; Malola, S.; Häkkinen, H. Evidence for Graphene Edges Beyond Zigzag and Armchair. *Phys. Rev. B: Condens. Matter Mater. Phys.* **2009**, *80*, 073401.
(26) Kunstmann, J.; Özdoğan, C.; Quandt, A.; Fehske, H. Stability of Edge States and Edge Magnetism in Graphene Nanoribbons. *Phys. Rev. B: Condens. Matter Mater. Phys.* **2011**, *83*, 045414.
(27) Dutta, S.; Pati, S. K. Edge Reconstructions Induce Magnetic and Metallic Behavior in Zigzag Graphene Nanoribbons. *Carbon* **2010**, *48*, 4409−4413.
(28) Deng, Q.; Zhao, J. Triggering One-Dimensional Phase Transition with Defects at the Graphene Zigzag Edge. *Nano Lett.* **2016**, *16*, 1244−1249.
(29) Wassmann, T.; Seitsonen, A. P.; Saitta, A. M.; Lazzeri, M.; Mauri, F. Structure, Stability, Edge States, and Aromaticity of Graphene Ribbons. *Phys. Rev. Lett.* **2008**, *101*, 096402.
(30) He, K.; Robertson, A. W.; Lee, S.; Yoon, E.; Lee, G.-D.; Warner, J. H. Extended Klein Edges in Graphene. *ACS Nano* **2014**, *8*, 12272−12279.
(31) Dang, J.-S.; Wang, W.-W.; Zheng, J.-J.; Nagase, S.; Zhao, X. Formation of Stone-Wales Edge: Multistep Reconstruction and Growth Mechanisms of Zigzag Nanographene. *J. Comput. Chem.* **2017**, *38*, 2241−2247.
(32) Jia, X.; Campos-Delgado, J.; Terrones, M.; Meunier, V.; Dresselhaus, M. S. Graphene Edges: A Review of Their Fabrication and Characterization. *Nanoscale* **2011**, *3*, 86−95.
(33) Huang, B.; Liu, M.; Su, N.; Wu, J.; Duan, W.; Gu, B.-l.; Liu, F. Quantum Manifestations of Graphene Edge Stress and Edge Instability: A First-Principles Study. *Phys. Rev. Lett.* **2009**, *102*, 166404.
(34) Rodrigues, J. N. B.; Gonçalves, P. A. D.; Santos, J. E.; Castro Neto, A. H. Thermodynamics of a Potts-Like Model for a Reconstructed Zigzag Edge in Graphene Nanoribbons. *Phys. Rev. B: Condens. Matter Mater. Phys.* **2013**, *87*, 134204.
(35) Cheng, Y. C.; Wang, H. T.; Zhu, Z. Y.; Zhu, Y. H.; Han, Y.; Zhang, X. X.; Schwingenschlögl, U. Strain-Activated Edge Reconstruction of Graphene Nanoribbons. *Phys. Rev. B: Condens. Matter Mater. Phys.* **2012**, *85*, 073406.
(36) van Ostaay, J. A. M.; Akhmerov, A. R.; Beenakker, C. W. J.; Wimmer, M. Dirac Boundary Condition at the Reconstructed Zigzag Edge of Graphene. *Phys. Rev. B: Condens. Matter Mater. Phys.* **2011**, *84*, 195434.
(37) Shu, H.; Chen, X.; Tao, X.; Ding, F. Edge Structural Stability and Kinetics of Graphene Chemical Vapor Deposition Growth. *ACS Nano* **2012**, *6*, 3243−3250.
(38) Wang, D.; Liu, Y.; Sun, D.; Yuan, Q.; Ding, F. Thermodynamics and Kinetics of Graphene Growth on Ni(111) and the Origin of Triangular Shaped Graphene Islands. *J. Phys. Chem. C* **2018**, *122*, 3334−3340.
(39) Artyukhov, V. I.; Hao, Y.; Ruoff, R. S.; Yakobson, B. I. Breaking of Symmetry in Graphene Growth on Metal Substrates. *Phys. Rev. Lett.* **2015**, *114*, 115502.
(40) Artyukhov, V. I.; Liu, Y.; Yakobson, B. I. Equilibrium at the Edge and Atomistic Mechanisms of Graphene Growth. *Proc. Natl. Acad. Sci. U. S. A.* **2012**, *109*, 15136−15140.
(41) Prezzi, D.; Eom, D.; Rim, K. T.; Zhou, H.; Lefenfeld, M.; Xiao, S.; Nuckolls, C.; Heinz, T. F.; Flynn, G. W.; Hybertsen, M. S. Edge Structures for Nanoscale Graphene Islands on Co(0001) Surfaces. *ACS Nano* **2014**, *8*, 5765−5773.
(42) Sinitsa, A. S.; Lebedeva, I. V.; Popov, A. M.; Knizhnik, A. A. Long Triple Carbon Chains Formation by Heat Treatment of Graphene Nanoribbon: Molecular Dynamics Study with Revised Brenner Potential. *Carbon* **2018**, *140*, 543−556.
(43) Tang, C.; Guo, W.; Chen, C. Structural and Mechanical Properties of Partially Unzipped Carbon Nanotubes. *Phys. Rev. B: Condens. Matter Mater. Phys.* **2011**, *83*, 075410.
(44) Song, B.; Schneider, G. F.; Xu, Q.; Pandraud, G.; Dekker, C.; Zandbergen, H. Atomic-Scale Electron-Beam Sculpting of near-Defect-Free Graphene Nanostructures. *Nano Lett.* **2011**, *11*, 2247−2250.
(45) Krasheninnikov, A. V.; Banhart, F. Engineering of Nanostructured Carbon Materials with Electron or Ion Beams. *Nat. Mater.* **2007**, *6*, 723−733.
(46) Kotakoski, J.; Santos-Cottin, D.; Krasheninnikov, A. V. Stability of Graphene Edges under Electron Beam: Equilibrium Energetics Versus Dynamic Effects. *ACS Nano* **2012**, *6*, 671−676.
(47) Cruz-Silva, E.; Botello-Méndez, A. R.; Barnett, Z. M.; Jia, X.; Dresselhaus, M. S.; Terrones, H.; Terrones, M.; Sumpter, B. G.; Meunier, V. Controlling Edge Morphology in Graphene Layers Using Electron Irradiation: From Sharp Atomic Edges to Coalesced Layers Forming Loops. *Phys. Rev. Lett.* **2010**, *105*, 045501.
(48) Kresse, G.; Furthmüller, J. Efficient Iterative Schemes for Ab Initio Total-Energy Calculations Using a Plane-Wave Basis Set. *Phys. Rev. B: Condens. Matter Mater. Phys.* **1996**, *54*, 11169−11186.
(49) Kresse, G.; Joubert, D. From Ultrasoft Pseudopotentials to the Projector Augmented-Wave Method. *Phys. Rev. B: Condens. Matter Mater. Phys.* **1999**, *59*, 1758−1775.
(50) Blöchl, P. E. Projector Augmented-Wave Method. *Phys. Rev. B: Condens. Matter Mater. Phys.* **1994**, *50*, 17953−17979.
(51) Perdew, J. P.; Burke, K.; Ernzerhof, M. Generalized Gradient Approximation Made Simple. *Phys. Rev. Lett.* **1996**, *77*, 3865−3868.
(52) Wang, H.; Wang, Y.; Lv, J.; Li, Q.; Zhang, L.; Ma, Y. Calypso Structure Prediction Method and Its Wide Application. *Comput. Mater. Sci.* **2016**, *112*, 406−415.
(53) Wang, Y.; Lv, J.; Zhu, L.; Ma, Y. Crystal Structure Prediction Via Particle-Swarm Optimization. *Phys. Rev. B: Condens. Matter Mater. Phys.* **2010**, *82*, 094116.
(54) Wang, Y.; Lv, J.; Zhu, L.; Lu, S.; Yin, K.; Li, Q.; Wang, H.; Zhang, L.; Ma, Y. Materials Discovery Via Calypso Methodology. *J. Phys.: Condens. Matter* **2015**, *27*, 203203.

https://dx.doi.org/10.1021/acs.jpclett.0c00525
J. Phys. Chem. Lett. 2020, 11, 3451−3457